AIP | Applied Physics Letters

Elegant Gaussian beams for enhanced optical manipulation

Christina Alpmann, Christoph Schöler, and Cornelia Denz

Citation: Applied Physics Letters **106**, 241102 (2015); doi: 10.1063/1.4922743
View online: http://dx.doi.org/10.1063/1.4922743
View Table of Contents: http://scitation.aip.org/content/aip/journal/apl/106/24?ver=pdfcov
Published by the AIP Publishing

Elegant Gaussian beams for enhanced optical manipulation

Christina Alpmann,[a] Christoph Schöler, and Cornelia Denz
Institute of Applied Physics, University of Muenster, Corrensstr. 2/4, 48149 Muenster, Germany

(Received 15 April 2015; accepted 2 June 2015; published online 15 June 2015)

Generation of micro- and nanostructured complex light beams attains increasing impact in photonics and laser applications. In this contribution, we demonstrate the implementation and experimental realization of the relatively unknown, but highly versatile class of complex-valued Elegant Hermite- and Laguerre-Gaussian beams. These beams create higher trapping forces compared to standard Gaussian light fields due to their propagation changing properties. We demonstrate optical trapping and alignment of complex functional particles as nanocontainers with standard and Elegant Gaussian light beams. Elegant Gaussian beams will inspire manifold applications in optical manipulation, direct laser writing, or microscopy, where the design of the point-spread function is relevant. © *2015 AIP Publishing LLC*. [http://dx.doi.org/10.1063/1.4922743]

Optical micromanipulation is a fast growing field with many applications in biophotonics and biomedicine.[1] Optical forces, which occur in highly focused beams, induce attractive forces on dielectric particles and allow to trap, move, and arrange them in three dimensional structures. A continuous decrease in size and simultaneous increase of the complexity of particle structures including nanocontainers, core-shell particles, and other functional materials (e.g., Janus particles and diatoms) evoke a recent development in the exploration of advanced light field shaping techniques to particularly tailor light with respect to the size, shape, and refractive index structure of the particle. Sophisticated light fields nowadays form an alternative branch in the field of optical micromanipulation and offer a high diversity of extended three-dimensional optical potential landscapes.[2–4]

While standard Gaussian beams as Hermite-, Laguerre-, and Ince-Gaussian beams as well as nondiffracting beams, including Bessel-, Mathieu-, and Airy-beams, have been introduced to optical micromanipulation in the past few years, we propose in this contribution the holographic modulation of the class of Elegant Gaussian beams[5] and their application to particle trapping. Elegant Gaussian beams are complementary to before mentioned complex light fields, due to their structural changing properties upon propagation. Although they have already been introduced in 1973 by Siegman,[6] they are predominantly known in theory but up to now have not been implemented in experimental physics. In recent publications, the vortex structure[7,8] of Elegant Gaussian beams, their ability to carry orbital angular momentum,[9,10] and Elegant vector wave packets[11] have been investigated theoretically. Also, the application to optical micromanipulation has remained on a conceptual, theoretical level: solely numerical simulations for Elegant Hermite-cosh-Gaussian beams[12,13] and partly coherent Elegant Laguerre-Gaussian beams[14] have been discussed. We demonstrate experimental holographic modulation of Elegant Gaussian beams for application in optical tweezers, analyze realized mode profiles, and discuss their advantageous potential to create high gradient forces at small scales, which are especially attractive to trap core-shell particles and nanocontainers.[15] In the first demonstration, the alignment of zeolite-L nanocontainer particles is shown.

Beside the common and well known solutions of standard Hermite-, Laguerre-, and Ince-Gaussian beams, Elegant Gaussian beams are alternative though less-known solutions of the paraxial wave equation, which can be solved in Cartesian (x, y, z), polar (r, ϕ, z), and elliptical (η, ξ, z) coordinates. However, in contrast to standard Gaussian beams, Elegant solutions exhibit a complex argument within the characteristic polynomials[6] determining their transverse mode structure and propagation behavior. For Elegant Hermite-Gaussian (eHG) beams

$$\mathrm{eHG} = \left(\frac{q_0}{q}\right)^{\frac{n_x+n_y}{2}} H_{n_x}\left(x\sqrt{\left(\frac{\mathrm{i}k}{2q}\right)}\right) H_{n_y}\left(y\sqrt{\left(\frac{\mathrm{i}k}{2q}\right)}\right) \times \frac{q_0}{q}\exp\left[-\frac{\mathrm{i}k}{2q}\left(x^2+y^2\right)-\mathrm{i}kz\right]. \quad (1)$$

The complex beam parameter q is defined via the beam radius $w(z)$ determined by $w^2(z) = w_0^2(1 + z^2/z_R^2)$ and the phase front curvature $R(z) = z + z_R^2/z$, $1/q = 1/R(z) - \mathrm{i}\lambda/(\pi w^2(z))$ with $q_0 = \mathrm{i}z_R$, the Rayleigh range $z_R = kw_0^2/2$, and the beam waist $w_0 = w(0)$. With the complex argument $x\sqrt{(\mathrm{i}k/2q)}$ in the Hermite polynomials H_n, an additional phase variation is introduced that modifies the usual Gaussian spherical phase front.[6] Therefore, Elegant Gaussian beams have a non-spherical phase front curvature and show structural instability, which means that the transverse beam profile of an Elegant beam changes during propagation. This loss of self-similarity by contrast with standard Gaussian beams can be seen in Figure 1, where transverse intensity and phase distributions of Elegant Hermite-Gaussian beams are shown in the near- as well as far-field. In comparison to standard Gaussian beams, where the transverse structure of the beam is scaled but maintained during propagation from near- to far-field, the structure of Elegant Gaussian beams changes remarkably. While the phase structure in the near-field is identical for standard and Elegant Gaussian beams, the intensity is located in outer parts of the transverse field of

[a]Electronic mail: c.alpmann@uni-muenster.de

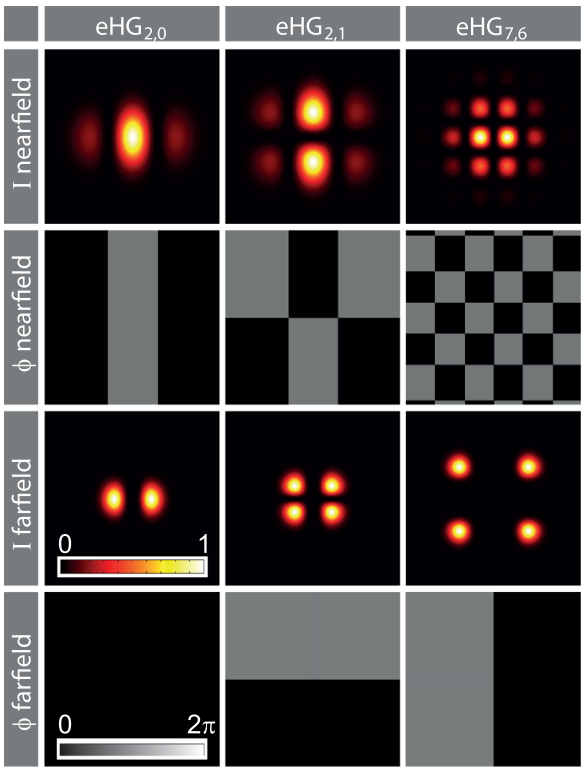

FIG. 1. Structural changing properties of Elegant Hermite-Gaussian beams: theoretical intensity and phase distributions of different eHG beams in the near-field at $z = 0$ (rows 1 and 2) and far-field (rows 3 and 4). Near- and far-field are independently scaled to enhance visibility of the structures.

standard beams but is centered in Elegant beams. In the far-field of Elegant beams, characteristic nodal lines of their transverse profiles disappear and lead to less structures located in the outer region.

In radial cylinder coordinates (r, ϕ, z), Gaussian beams are characterized by generalized Laguerre-Gaussian polynomials L_p^l with l and p being the azimuthal and radial mode index, respectively. Elegant Laguerre-Gaussian beams

$$\begin{aligned} \mathrm{eLG} &= \left(\frac{q_0}{q}\right)^{\frac{p+|l|}{2}} L_p^l\left(\frac{\mathrm{i}k}{2q}r^2\right)\exp[\mathrm{i}l\phi] \\ &\quad \times \frac{q_0}{q}\exp\left[-\frac{\mathrm{i}k}{2q}r^2 - \mathrm{i}kz\right] \end{aligned} \tag{2}$$

have a helical phase structure similar to standard Laguerre-Gaussian beams. This means they carry optical orbital angular momentum proportional to the topological charge l giving the number of intertwined helical wavefronts. The handedness of these so called optical vortices is defined by the sign of l, and the corresponding modes are denoted as eLG^+ and eLG^-. Beside these helical modes, *even* and *odd* eLG modes

$$\begin{aligned} \mathrm{eLG}^e &= \frac{1}{2}(\mathrm{eLG}(l) + \mathrm{eLG}(-l)) \\ &= \left(\frac{q_0}{q}\right)^{\frac{p+|l|}{2}} L_p^l\left(\frac{\mathrm{i}k}{2q}r^2\right)\cos(l\phi) \\ &\quad \times \frac{q_0}{q}\exp\left[-\frac{\mathrm{i}k}{2q}r^2 - \mathrm{i}kz\right], \end{aligned} \tag{3}$$

$$\begin{aligned} \mathrm{eLG}^o &= \frac{1}{2\mathrm{i}}(\mathrm{eLG}(l) - \mathrm{eLG}(-l)) \\ &= \left(\frac{q_0}{q}\right)^{\frac{p+|l|}{2}} L_p^l\left(\frac{\mathrm{i}k}{2q}r^2\right)\sin(l\phi) \\ &\quad \times \frac{q_0}{q}\exp\left[-\frac{\mathrm{i}k}{2q}r^2 - \mathrm{i}kz\right] \end{aligned} \tag{4}$$

provide similar to standard Laguerre-Gaussian beams petal like mode structures in the focal plane. Figure 2 shows intensity and phase distributions of the near- $(z = 0)$ and far-field of helical, even, and odd Elegant Laguerre-Gaussian beams. The propagation behavior is similar to Elegant Hermite-Gaussian beams.

We propose to generate Elegant Gaussian beams by a spatial light modulator (SLM) using a combined holographic amplitude and phase modulation technique,[16] which allows to encode a complex field $E = A\exp(\mathrm{i}\varphi)$ into a phase only function

$$\Phi = \exp[\mathrm{i}A'(\varphi + \varphi_b - A'\pi)]. \tag{5}$$

Φ reproduces the desired complex field in the first diffraction order, which is spatially separated from other diffraction orders by the linear function φ_b. A corrected amplitude information A' is determined using a look up table defined by $A = \mathrm{sinc}(1 - A')$ for $A, A' \in [0, 1]$ to modulate the desired amplitude information.

For many applications, micro- and nanostructured light fields are focused by a microscope objective (MO) into the sample plane (SP) of an inverted microscope (see Figure 3).

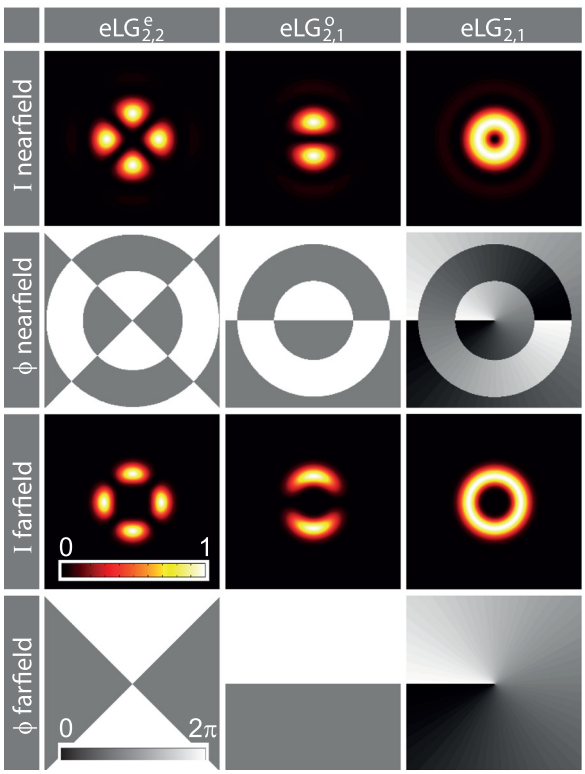

FIG. 2. Structural changing properties of Elegant Laguerre-Gaussian beams: theoretical intensity and phase distributions of different eLG beams in the near-field at $z = 0$ (rows 1 and 2) and far-field (rows 3 and 4). Near- and far-field are independently scaled to enhance visibility of the structures.

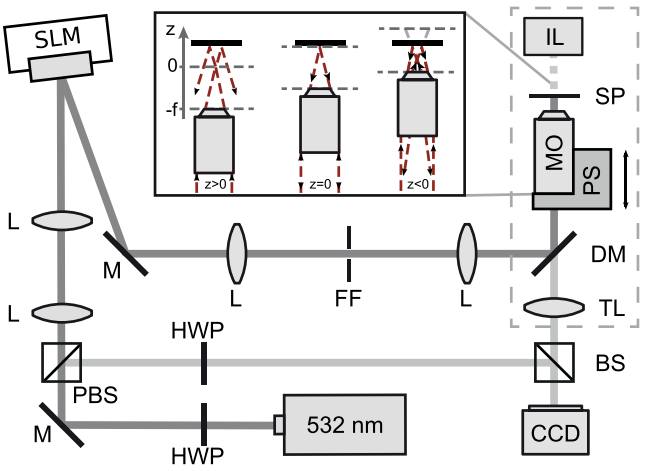

FIG. 3. Setup sketch for the holographic modulation of Elegant Gaussian beams on the micron size. The inset illustrates the movement of the MO to measure z-stacks of the beam. FF: Fourier filter, DM: dichroic mirror, HWP: half wave plate, IL: illumination (optional), L: lens, M: mirror, MO: microscope objective, PS: piezo scanner, (P)BS: (polarizing) beam splitter, SLM: spatial light modulator, SP: sample plane, and TL: tube lens.

Solely, the first diffraction order is transmitted by a diaphragm in a Fourier plane of the SLM, before the light is reflected by a dichroic mirror (DM) into the microscope and imaged onto the back focal plane of the MO. In this geometry, a Fourier hologram is required for the far-field modulation of the focused light field. For Elegant Gaussian beams, the Fourier transformation is given by[17]

$$\mathcal{F}(\mathrm{eHG})(\eta,\xi,z) \propto \left(\frac{k\eta}{z}\right)^{n_x}\left(\frac{k\xi}{z}\right)^{n_y} \times \exp\left[-\frac{w_0^2}{4}\left(\frac{k^2\eta^2}{z^2}+\frac{k^2\xi^2}{z^2}\right)\right], \quad (6)$$

$$\mathcal{F}(\mathrm{eLG})(\rho,\theta,z) \propto \exp\left[-\frac{w_0^2}{4}\rho^2\right]\rho^{2p+|l|}\begin{pmatrix}\exp[\mathrm{i}l\theta]\\ \cos(l\theta)\\ \sin(l\theta)\end{pmatrix}. \quad (7)$$

To analyze the modulated light field, a mirror placed in the focal plane of an oil-immersion MO reflects the light backwards to the camera ports of the microscope where the spatial intensity profile of the beam is directly imaged onto a CCD. Alternatively, the phase information can be reconstructed out of the interference pattern of the modulated beam with a tilted plane reference wave.[18] To correct for spatial inhomogeneities of the SLM and the setup in general, a wavefront correction[19] has been measured for our setup, which is displayed on the modulator together with the phase only function Φ. This method allows for high fidelity modulation of submicron structured higher order modes and other complex light fields.

Experimental results for intensity and phase measurements taken in the focal plane of the MO are shown in Figure 4 for Elegant Hermite- and Laguerre-Gaussian beams. Single structures provide feature sizes smaller than 400 nm (see e.g., $\mathrm{eHG}_{7,6}$). Except for small spatial inhomogeneities which can be explained by an elliptical beam profile of the laser, all intensity distributions coincide well with theory (compare Figures 1 and 2 with Fig. 4). Holographic phase measurements reproduce the theoretical predictions except for an irrelevant relative phase shift in regions of sufficient intensity. If the contrast of the interference fringes is too low, random phase values are obtained, as seen in the outer parts of the phase images in Fig. 4. The phase of a fundamental Gaussian beam was used as reference and subtracted from the particular beam.

To analyze the propagation behavior of Elegant Gaussian beams, the MO was shifted with respect to the mirror by a piezo stage to take a z-stack of transverse intensity profiles. Moving the objective upwards, as indicated in the inset of Fig. 3, scans the light field from $z_{start} > 0$ to $z_{end} < 0$ as the light is reflected by a mirror in the sample plane of the inverted microscope. We used 100 nm steps of the piezo stage to scan the beams in 200 nm longitudinal shifts. Three-dimensional theoretical and experimental intensity profiles are shown for eHG and eLG beams in Fig. 5. 3D plots are obtained by an overlay of isosurface and contour plots, wherefore each image has been normalized separately. On the right, images taken at $z = 0\,\mu$m and $z = 3\,\mu$m are shown. For the Hermite-Gaussian beam, the characteristic change in the beam profile during propagation can be well seen.

As the light was focused by a high numeric aperture oil-immersion objective (NA = 1.3), the Fourier hologram contained additional terms to correct for spherical aberrations.

High angle far-field distributions of Elegant Gaussian beams not only result in high intensity peaks in the center of the mode in the near-field but also enhance optical gradient forces $F_{\mathrm{grad}} \propto \nabla I$ acting on transparent microparticles, as can be seen from the profile of the normalized intensity gradient $\nabla I/I_{\mathrm{mean}}$ shown in Fig. 6. This means that Elegant Gaussian beams might be better suited for optical manipulation to trap and align particles within

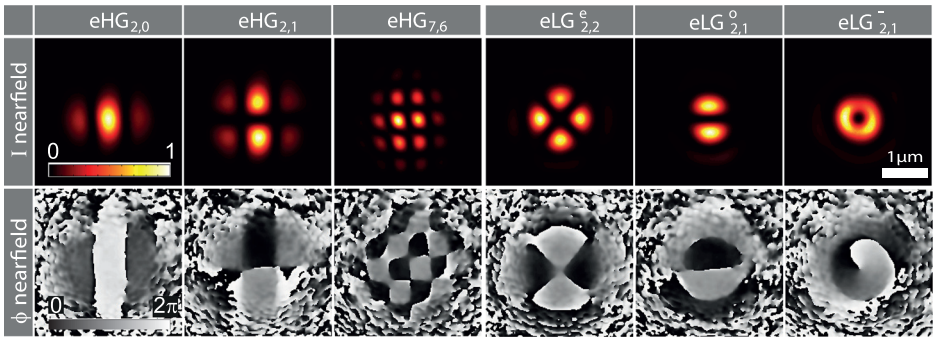

FIG. 4. Experimental intensity and phase measurements of holographically generated Elegant Hermite-and Laguerre-Gaussian beams in the focal plane of a microscope objective.

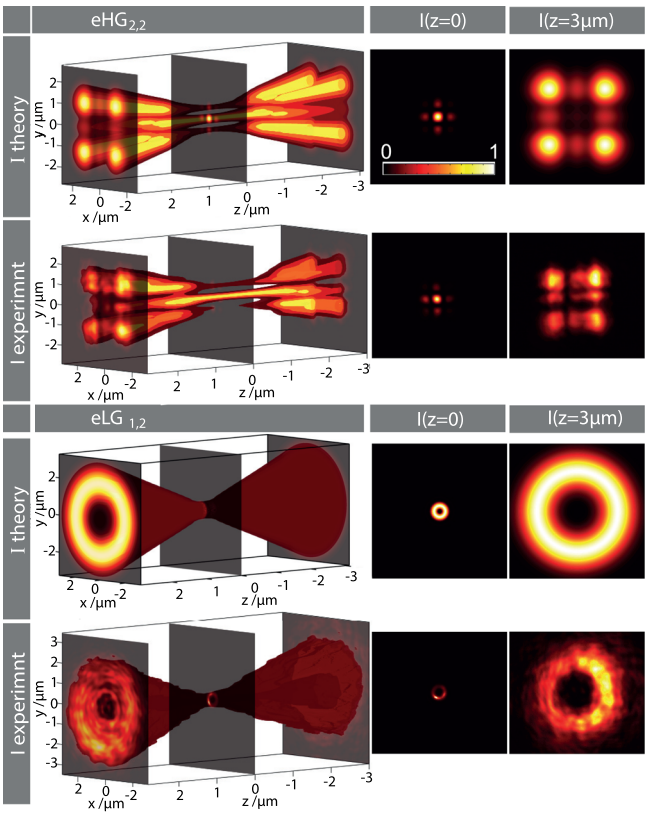

FIG. 5. Three dimensional theoretical and experimental intensity profiles of Elegant Hermite- and Laguerre-Gaussian beams visualized by isosurface and contour plots.

submicron structured profiles. In the first experiment, we compared trapping and alignment of zeolite-L nanocontainer particles for standard and Elegant Gaussian beams. Zeolite-L crystals are nanoporous alumosilicates containing one-dimensional nanochannels, which are able to accommodate guest molecules as drugs or dyes.[20] From former experiments, it is known that zeolites align with their long axis parallel to the propagation direction of light in standard holographic optical tweezers (HOT).[15] With two or more traps, they can be rotated and have been used, e.g., as suitable building blocks to form bio-hybrid micro-robots.[21] We now investigate their orientation and alignment in higher order standard and Elegant Gaussian beams and compare both results with the alignment in the fundamental Gaussian beam, which is typically used in HOT. Fig. 6 shows the experimental intensity images of the focal plane of the light field, bright-field images of the trapped zeolite, and sketches to illustrate zeolite alignment. The orientation of the nanocontainer is similar in the fundamental and the Elegant Gaussian beam (100× MO, NA = 1.4), as in both cases, the long axis is aligned in the direction of light propagation. But as the geometry of the Elegant Gaussian light field better matches the geometry of the particle, it aligns more straightly compared to the fundamental Gaussian beam where a small tilt of the particle with the beam axis can be observed. In opposite to the parallel alignment, the standard Hermite Gaussian beam of the same order as the Elegant Gaussian beam leads to a perpendicular orientation of the zeolite with respect to the direction of propagation of the light (60× MO, NA = 1.49). The reason for this is the relative intensity distribution of the beam, where the highest intensity peaks are located in the outer lopes of the standard beam and therefore create an optical potential, which can be compared to the case of two or three traps in HOT. During the experiment, we switched several times between different beams and observed that these characteristic alignments are reproducible.

In conclusion, Elegant Gaussian beams as alternative solutions of the paraxial Helmholtz equation provide interesting changes of their transverse structure during propagation due to their instability caused by complex arguments of their characteristic polynomials. To overcome the nonavailability of Elegant beams in laser applications, we proposed a holographic modulation technique to generate submicron structured Elegant Gaussian beams within the focal plane of high NA microscope objective. After measuring a phase correction for our setup, the combined amplitude and phase modulation technique allows to generate high fidelity complex light modes. We analyzed the beam profiles of Elegant Hermite- and Laguerre-Gaussian modes and showed that the intensity and phase measurements are in excellent agreement with theoretical predictions. Moreover, we measured *z*-stacks to visualize the characteristic changes of Elegant Gaussian light fields during propagation and discussed the influence of spherical aberrations on Elegant Gaussian beams. We compared the alignment of zeolite-L nanocontainers for the fundamental, Elegant, and standard Gaussian light modes and propose to use the high angle contributions in the far field of Elegant Gaussian beams to enhance trapping forces in optical micro manipulation.

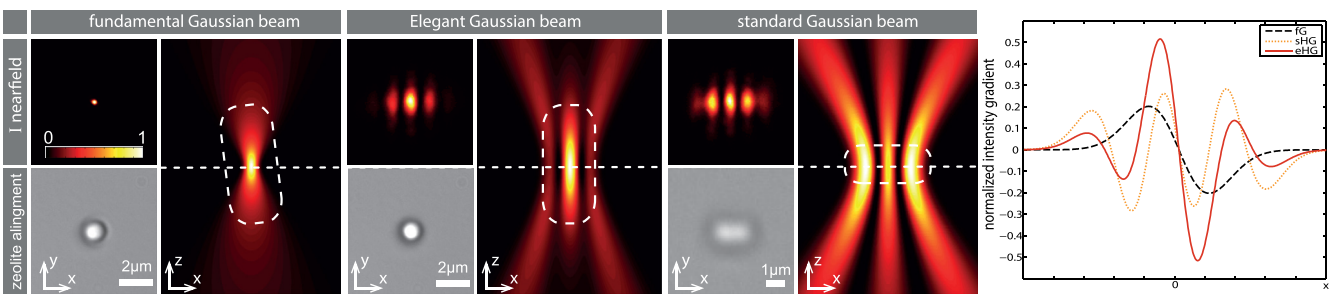

FIG. 6. Optical alignment of zeolite nanocontainer particles within (from left to right) a fundamental Gaussian beam, an Elegant Hermite-Gaussian beam ($eHG_{2,0}$), and a standard Hermite Gaussian beam ($sHG_{2,0}$). For each case, the experimental intensity image of the focal plane of the trapping light field, a bright field illumination image of the trapped zeolite, and a sketch to illustrate the zeolite alignment are shown. On the right, profiles along the horizontal white dashed lines of the intensity gradient $\nabla I/I_{\mathrm{mean}}$ are shown.

The authors thank the German research foundation (DFG) for financial support in the frame of the German-Chinese Transregional Research Project TRR61, A. Stilgoe (University of Queensland, Australia) for discussions about spherical aberration corrections and A. Studer and T. Buscher (both Organic Chemistry Institute, University of Muenster) for providing zeolite-L crystals.

[1]F. M. Fazal and S. M. Block, Nat. Photonics **5**, 318–321 (2011).
[2]M. Woerdemann, C. Alpmann, M. Esseling, and C. Denz, Laser Photonics Rev. **7**, 839–854 (2013).
[3]K. Dholakia and T. Čižmár, Nat. Photonics **5**, 335–342 (2011).
[4]M. Padgett and R. Bowman, Nat. Photonics **5**, 343–348 (2011).
[5]S. Saghafi and C. J. R. Sheppard, J. Mod. Opt. **45**, 1999–2009 (1998).
[6]A. E. Siegman, J. Opt. Soc. Am. **63**, 1093–1094 (1973).
[7]I. Martinez-Castellanos and J. C. Gutiérrez-Vega, J. Opt. Soc. Am. A **30**, 2395–2400 (2013).
[8]W. Nasalski, Appl. Phys. B **115**, 155–159 (2014).
[9]D. Lopez-Mago, J. Davila-Rodriguez, and J. C. Gutiérrez-Vega, J. Opt. **15**, 125709 (2013).
[10]V. V. Kotlyar and A. A. Kovalev, J. Opt. Soc. Am. A **31**, 274–282 (2014).
[11]W. Nasalski, Opt. Lett. **38**, 809–811 (2013).
[12]Z. Liu and D. Zhao, Opt. Express **20**, 2895–2904 (2012).
[13]Z. Liu, K. Huang, and D. Zhao, Opt. Lasers Eng. **51**, 761–767 (2013).
[14]C. Zhao and Y. Cai, Opt. Lett. **36**, 2251–2253 (2011).
[15]M. Woerdemann, S. Gläsener, F. Hörner, A. Devaux, L. De Cola, and C. Denz, Adv. Mater. **22**, 4176 (2010).
[16]J. A. Davis, D. M. Cottrell, J. Campos, M. J. Yzuel, and I. Moreno, Appl. Opt. **38**, 5004–5013 (1999).
[17]A. Wünsche, J. Opt. Soc. Am. A **6**, 1320–1329 (1989).
[18]M. Esseling, *Photorefractive Optoelectronic Tweezers and their Applications* (Springer, 2015).
[19]T. Čižmár, M. Mazilu, and K. Dholakia, Nat. Photonics **4**, 388–394 (2010).
[20]D. Bruhwiler and G. Calzaferri, Microporous Mesoporous Mater. **72**, 1–23 (2004).
[21]Á. Barroso, S. Landwerth, M. Woerdemann, C. Alpmann, T. Buscher, M. Becker, A. Studer, and C. Denz, J. Biomed. Microdevices **17**, 26 (2015).